ECS Transactions, 2 (5) 15-25 (2006)
10.1149/1.2204875, copyright The Electrochemical Society

# High-resolution spectroscopic measurements of InGaAs/GaAs self-assembled quantum dots

J. J. Berry, Martin J. Stevens, R. P. Mirin, and K. L. Silverman
*National Institute of Standards and Technology, Boulder, Colorado 80305*

We report development of two absorption-based spectroscopic methods that have been adapted from atomic physics techniques to elucidate the basic physical properties of InGaAs/GaAs self-assembled quantum dots (SAQDs). Absorptive spectroscopic measurements allow the examination of the SAQDs optical transitions free from carrier relaxation effects. In addition, we employ these techniques to study SAQDs' optical transition with a level of spectral resolution not available using ultra-fast techniques. The first of the two approaches we discuss is cavity ring-down spectroscopy (CRDS), which permits an absolute measurement of absorption. We report on initial application of CRDS to SAQDs and present an assessment based on these measurements for single SAQD spectroscopy using this technique. The second method, spectral hole burning, is applied to SAQDs in a semiconductor ridge waveguide and permits the homogeneous linewidth of the SAQDs to be separated from the broad inhomogeneous spectrum.


## I. INTRODUCTION

Self-assembled quantum dots (SAQDs) are semiconductor nanostructures composed of defect-free crystalline material that result in true three-dimensional confinement in a semiconductor heterostructure. At low temperatures the SAQDs three-dimensional confinement results in a density of states and optical transitions analogous to those found in atomic systems. Due to these similarities SAQD are often referred to as 'artificial atoms'. Although numerous classes of quantum dots exist, the InGaAs/GaAs SAQDs considered here maintain their three-dimensional confinement at room temperature, despite considerable broadening of the optical transitions due to phonon interactions. These properties along with their compatibility with other III-V based microelectronics, make InGaAs SAQDs of particular interest for improving traditional optoelectronic devices. The broad inhomogeneous linewidth of SAQD ensembles, resulting from slight differences in the confinement potential make them useful for lasers, photodetectors and other low power optoelectronic applications. In addition, the narrow SAQD homogeneous linewidth makes individual quantum dots of considerable interest in quantum optics applications such as secure optical communication and linear-optical quantum computing. Experimental demonstrations have shown InGaAs/GaAs SAQDs are both efficient single-photon emitters and potentially important nonclassical light sources (1, 2). This wide variety of device application makes the basic physical properties of SAQDs of increasing importance.

The majority of experimental studies to date have investigated emission from either ensembles or single SAQDs (3). Optical studies of SAQDs using absorption measurements, while potentially more insightful, require more sensitive experimental probes. In this report we discuss two approaches to performing sensitive resonant absorption measurements on InGaAs SAQD ensembles undertaken in our group. These measurements allow the optical transitions in the SAQDs to be examined free from carrier relaxation effects. The extremely broad inhomogeneous lineshapes of SAQD ensembles have precluded the use of linear optical measurements to resolve the relatively narrow homogeneous linewidth. Several groups have used time domain measurements to perform absorption measurements by measuring the decay of the 'photon echo' after ultrafast excitation, with considerable success (4). However, these techniques have limited spectral resolution due to the inherent bandwidth, typically 1 nm or more, of the optical probes employed. Here we will discuss cavity-ringdown and spectral hole burning spectroscopy, which are both high-resolution techniques adapted from atomic physics and chemistry. Both techniques employ narrow frequency ($< 10$ MHz) continuous wave sources, which results in enhanced spectral resolution.

## II. CAVITY RING-DOWN SPECTROSCOPY

One method for performing sensitive absorption measurements is cavity ring-down spectroscopy (CRDS). As the name suggests, this technique employs an optical resonator in which light is inserted. Once inserted the decay, or ring-down, of the transmitted optical power through the resonator is

studied. By examining the cavity ring-down with and without the presence of an absorber, or equivalently, on and off the absorption resonance, the change in cavity dynamics can be observed and analyzed. The cavity ring-down may be described by the time dependent number of photons $N_p(t)$ in the cavity, which can be described by a simple exponential $N_p(t) = N_0 e^{-t/\tau}$. The cavity time constant $\tau$ in the presence of an absorber is then given as

$$\frac{1}{\tau} = \left[(1-S) + \alpha \frac{2F}{\pi} L_i\right] \frac{c}{2d}, \qquad [1]$$

where $L_i$ is the interaction length between the photon and the absorber, $\alpha$ is the absorption coefficient which is enhanced by the factor $(2F/\pi)$, and $(d)$ is the length of the cavity. The empty-cavity finesse F is given as

$$F = \frac{\pi (S)^{\frac{1}{4}}}{1-(S)^{\frac{1}{2}}}, \qquad [2]$$

where $S = R_1 R_2$ is the cavity survival factor for a two-mirror cavity, and $R_1$ and $R_2$ are the individual mirror reflectivities. Data showing the cavity decay for a test cavity is shown in FIG. 1. The linearity of the curves plotted on a logarithmic scale verifies that the decay is exponential in form. Fits to the data permit the calculation of reflectivities, which are also indicated in the figure.

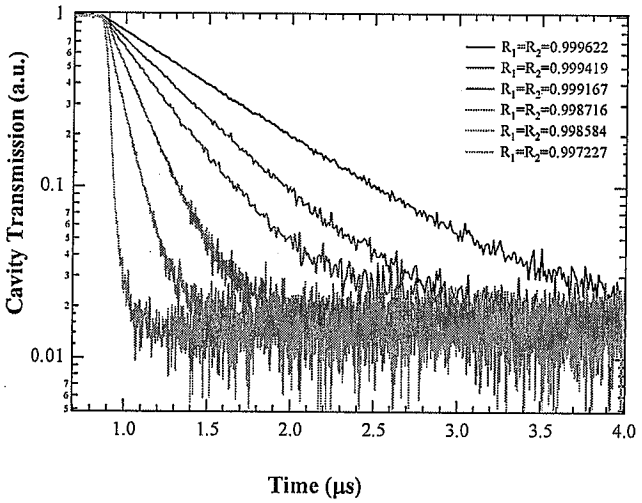


FIG. 1: Figure shows continuous wave cavity ringdown data for a test cavity composed of two dielectric mirrors. Data clearly follow the exponential decay given by $N_p(t) = N_0 e^{-t/\tau}$ along with equations [1] and [2] over a range of reflectivities.

We first applied this general CRDS approach to InGaAs SAQDS in a low-finesse pulsed incarnation known as multi-bounce absorption spectroscopy or pulsed cavity-ringdown spectroscopy (PRDS), to make absolute measurements of the SAQD ensemble absorption coefficient. The samples for this and all subsequent measurement were grown using molecular beam epitaxy (MBE) on GaAs substrates. For these measurements a single undoped InGaAs SAQD layer was incorporated into a AlGaAs/GaAs/AlGaAs ridge waveguide shown, schematically in FIG. 2. The cleaved waveguide facets serve as low reflectivity ($R_1, R_2 \sim 0.3$) cavity mirrors. While this approach does not permit a high degree of spectral resolution, and due to the low cavity finesse has virtually no cavity enhancement of the absorption, the technique is insensitive to the input/output coupling to the waveguide. The elimination of the coupling efficiency from the measurement removes a major contribution to the experimental uncertainty, making it possible to accurately measure the SAQD dipole moment. Reference (5) gives detailed information about measurements made using this technique, in addition to details regarding the analysis and results outside the purview of this paper. However, from these low-finesse CRDS measurements, we can estimate the sensitivity required to detect the SAQD

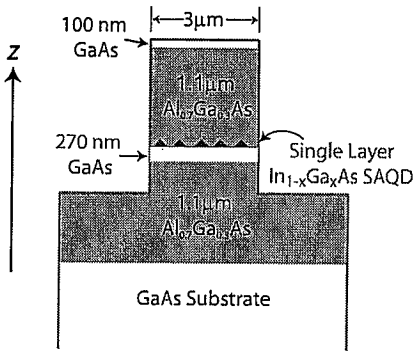


FIG. 2: Schematic of sample structures. The $z$ axis is the growth direction for the sample

ground state absorption when the SAQDs are illuminated at normal incidence. We estimate a peak modal loss of 4 $cm^{-1}$ and a confinement factor of 36, which yields a material absorption coefficient of 144 $cm^{-1}$. This, combined with a typical SAQD thickness of ~10 nm, yields an optical modulation of only $\sim 1\times10^{-4}$ for a single SAQD layer. Based on this, we do not expect standard linear transmission measurements to provide the required signal to noise ratio for examination of a single layer of SAQDs, much less an isolated SAQD. We can, however, obtain this level of sensitivity with continuous wave CRDS (CWCRDS) by utilizing a high finesse optical cavity. This method is a standard technique for the examination of transitions in atomic and molecular vapors. In the remainder of this section we will discuss our initial experiments in the application of CWCRDS to high resolution SAQD spectroscopy.

In our CWCRDS measurements the optical excitation is provided by a CW Ti:Sapphire laser stabilized to a fixed reference cavity using a Pound-Drever-Hall technique (6). The cavity stabilization results in a laser linewidth of less than 500 kHz. The narrow-frequency laser light is then guided via a single-mode polarization-maintaining fiber to the experimental cavity. This cavity is composed of two portions. The first half of the cavity consists of a conventional dielectric mirror, with a high-reflectivity coating centered at a wavelength of 1.064 $\mu$m, attached to a piezoelectric transducer, and a low thermal expansion glass spacer. The second half of the cavity consists of the sample mirror, which is mounted in a conventional mirror mount on a translation stage. The complete sample and reference assembly is mounted on a lead brick to provide a rigid link while permitting different portions of the sample mirror to be examined. The resulting experimental cavity has a length of $d = 0.704$ m. The dielectric mirror has a radius of curvature of 1 m, giving the cavity a laser beam waist at the sample mirror of $\sim 285$ $\mu$m. The cavity loading is performed by sweeping the cavity resonance frequency across the fixed laser frequency, then switching off the input beam using an acousto-optic modulator. The cavity transmission is directed into a commercial InGaAs photodetector with 125 MHz of bandwidth, and the ring-down signal is recorded by a digitizing oscilloscope. The input power to the experimental cavity is fixed at approximately 200 $\mu$W for all the measurements presented here. The sample mirrors for all these experiments are MBE grown distributed Bragg reflectors (DBRs) consisting of 25-period semi-insulating heterostructures AlAs/GaAs on 3" semi-insulating GaAs substrates. The first DBRs examined were designed with high reflectivity centers at $\lambda = 1.01$ $\mu m$ with (3/4) $\lambda$ and full $\lambda$ thickness GaAs cladding layers to manipulate the node and anti-nodes of the electric field relative to the DBR. The cavity finesses resulting from pairing these sample mirrors with our curved dielectric mirror are shown in FIG. 3(a), with theoretical cavity finesses shown in FIG. 3(b).

As previously mentioned, in traditional ring-down measurements the absorber is typically in the gas phase, and its introduction into the optical cavity can be accomplished in a straightforward manner. In the case of our SAQDs the inclusion of the SAQDs into the optical cavity is accomplished by integrating the SAQDs directly onto the MBE-grown DBR. While this allows the introduction

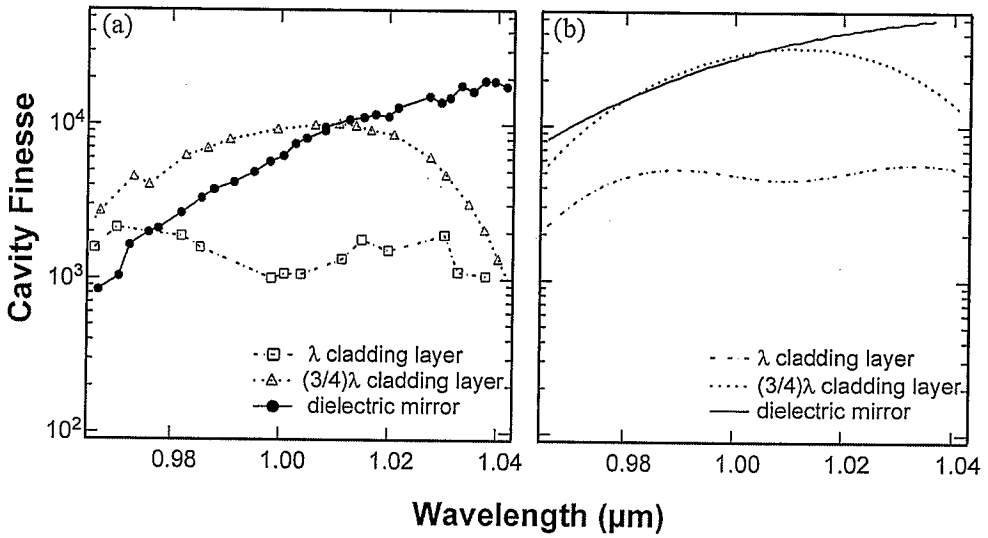


FIG. 3: Experimental and theoretical analysis of cavity finesses. Dielectric mirrors have a high-reflectivity coating center wavelength of $\lambda \sim 1.064$ $\mu$m, while the DBR samples were designed with a center wavelength of $\lambda \sim 1.010$ $\mu$m. Panel (a) shows cavity finesses determined by ring-down measurements with a cavity waist at the sample mirror of $\omega_0 = 285$ $\mu$m (error bars are within symbols). Panel (b) shows cavity finesses calculated from the modeling of the dielectric and DBR mirrors. In all cases the qualitative agreement in curve shapes between theory and experiment is quite good, despite the clear quantitative difference in absolute value of the finesse.

of the SAQD into the optical cavity, it makes the separation of DBR reflectivity from the SAQD absorption difficult. In these ensemble measurements the introduction of the SAQDs is accomplished by integrating the SAQD layer into a GaAs cladding layer of our GaAs/AlAs DBR heterostructures. By tuning the electric field penetration we can engineer the heterostructures to maximize the electric field overlap with the SAQD absorbers at the center wavelength of the measurements. In addition, we have added a density variation into the SAQD layer by stopping the substrate rotation during the SAQD deposition. This variation in the SAQD density across the wafer is verified by photoluminescence (PL) measurements performed at a fixed excitation power, and is shown in FIG. 4. Also shown in FIG. 4 are spectrophotometer-based measurements of the cavity mirrors. The spectrophotometer measurements show the overlap of the reflectivity spectra of the curved dielectric mirror and DBR mirror with the emission spectra of the SAQDs embedded in the $(3/4)\lambda$ cladding layer. While less precise, the spectrophotometer measurements allow the characterization of the mirrors away from the high-reflectivity center, where the reflectivity is too low to easily examine with the CWCRDS measurements. From these data we find that the SAQD/DBR structure's reflectivity is centered at $\lambda = 0.991$ $\mu$m. Results of ring-down measurements on the same sample, characterized in FIG. 4, are shown in FIG. 5. As FIG. 5 indicates, the wavelength dependence of the ring-down was taken at several different positions on the wafer. A clear dependence of the sample reflectivity on cavity waist location is observed in the data. While the center reflectivity blue-shifts by 15 nm or more in our DBR samples, the blue-shifts are found to be symmetric about the wafer center. In contrast, the ring-down data clearly indicate a monotonic increase in the cavity finesse and survival factor, which are correlated with the decrease in the SAQD number density across the sample. Note that the cavity survival factor, and hence the cavity finesse, is considerably lower than that found for the DBR shown in FIG. 3, which does not contain SAQDs . This reduction in the DBR sample reflectivity and cavity finesse lowers the absorption sensitivity. While the reduction is due in part to the SAQD contributions, other factors relating to the DBR portion of the sample, such as interfacial roughness and lateral spatial non-uniformities in the DBR layers, may also be significant contributions. Unlike the PRDS measurements previously discussed, in the case of CWCRDS measurements, the details of the mirror reflectivity are integral to understanding the absorption properties of the SAQDs that have been incorporated into the cavity. As a result, all non-SAQD sources of loss must

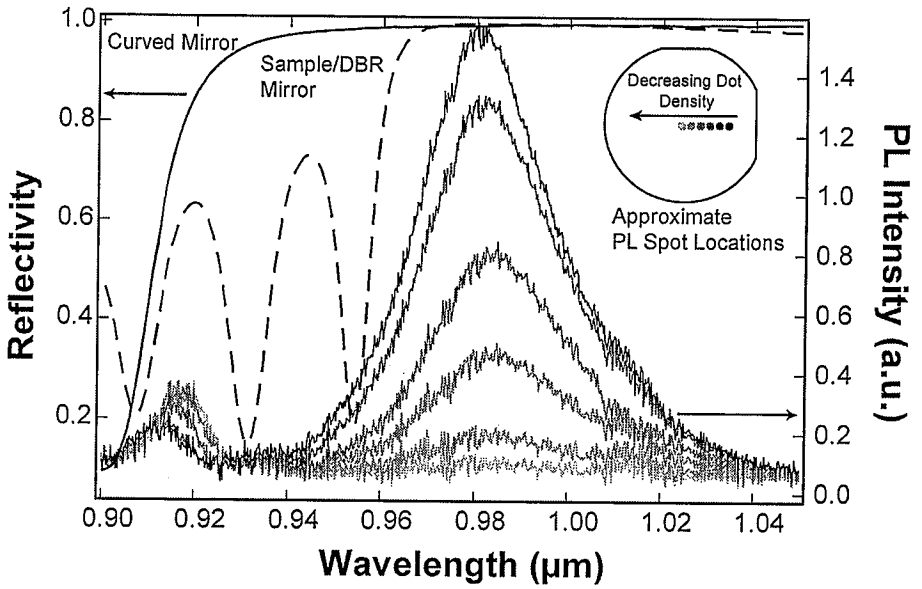


FIG. 4: Spectrophotometer-based measurements on dielectric curved mirror and DBR mirror with SAQDs integrated into the GaAs cap layer (left axis). Photoluminescence (PL) spectra as a function of wafer position at fixed pump power. PL spectra were taken with a 200 $\mu$W pump at 532 nm and show the spatial variation in the SAQD density. Inset shows PL spot locations on wafer relative to wafer flat.

be accounted for if meaningful SAQD absorption data are to be extracted. Currently examination of what physical mechanisms limit the reflectivity of our DBRs is in progress.

Based on these measurements we may examine the requirements for the observation of absorption from a single SAQD. The minimum measurable absorption $\alpha_{min}$ in a cavity is given by

$$\alpha_{min} = \frac{\pi}{2FL_i}\left(\frac{\delta P_t}{P_t}\right), \qquad [3]$$

where $P_t$ is the transmitted power $\delta P_t$ is the minimum detectable transmitted power contrast, and $L_i$ is again the photon/absorber interaction length. Experimentally we find a typical value for $(\delta P_t/P_t) \sim 0.015$, which is determined in part by the experimental noise from the photodetector and digitization of the ring-down signal (7). For our best reflectors without SAQDs the calculated $\alpha_{min}$ is found to be $3.35 \times 10^{-7}$ cm$^{-1}$. This $\alpha_{min}$ indicates that the current experiment should be able to detect a single absorber with a dipole moment of $2.3 \times 10^{-27}$ C $\cdot$ m (707 debye) at a center wavelength of 1.01 $\mu$m. In comparison a single InGaAs SAQD is expected to have a dipole moment of $1.04 \times 10^{-29}$ C $\cdot$ m (31 Debye) (8) and a corresponding absorption of $6.53 \times 10^{-10}$ cm$^{-1}$. As a result, our experimental sensitivity needs an improvement of at least a factor of 500 in order to effectively perform single SAQD spectroscopy. In order to obtain the additional sensitivity required for single SAQD absorption and the examination of the SAQD homogeneous linewidth using this measurement technique, the dynamic range of the measurement must be improved via improvements in the detection and/or cavity finesse along with a commensurate increase in digitization. Advanced ring-down based techniques such as noise-immune cavity-enhanced optical heterodyne spectroscopy or heterodyne ring-down techniques, as outlined by Ye *et al.* (9, 10) will likely be required for detailed investigations of a single SAQD absorption line using this cw technique. Other possibilities, such as using a modified PRDS approach, will also have significant technical hurdles. Despite the sensitivity limits of our current CRDS SAQD measurements we have demonstrated its potential for applications to nanostructured material systems and are able to assess its future potential in this area.

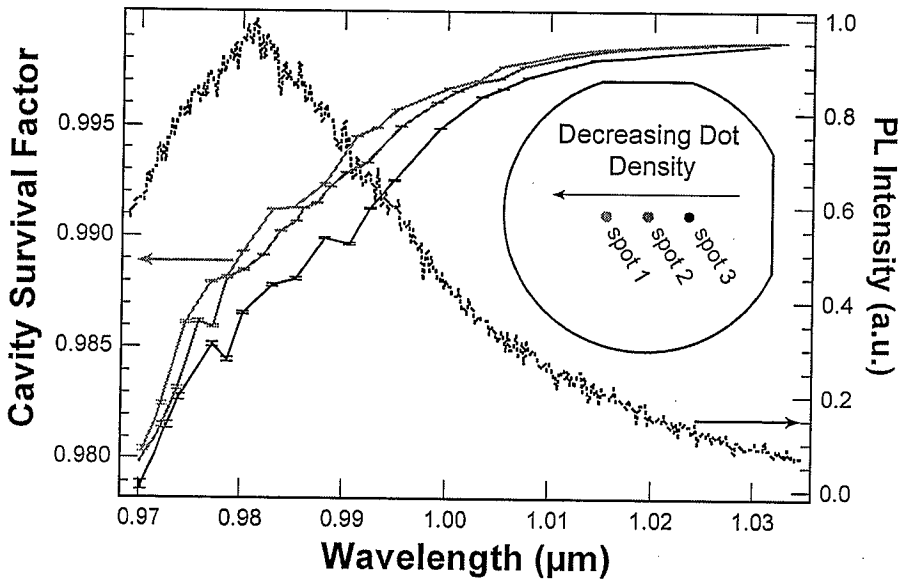


FIG. 5: Cavity survival factor (left axis) as determined by cavity ring-down measurements on quantum dot ensembles integrated with SAQD photoluminescence spectra (right axis). Decrease in the survival factor as a function of the spot location unambiguously shows evidence of SAQD absorption.

## III. SPECTRAL-HOLE BURNING

A second approach to narrow frequency spectroscopy, which we successfully applied to SAQDs, is continuous wave spectral hole burning (CWHB). In a fashion analogous to the ringdown technique, spectral hole burning measurements in a semiconductor ridge wave guide have been performed using time domain techniques, which place limits on the spectral resolutions of these experiments. In contrast the CWHB measurements permit the examination of narrow spectral features limited only by the inherent bandwidth of the lasers. While this technique has been applied to myriad atomic studies and more recently to solid state systems such as CdSe nanocrystals (11), its application to the InGaAs SAQD system in our experimental geometry represents a novel application of this experimental method. For these measurements we use a collinear pump-probe arrangement to examine a single InGaAs/GaAs SAQD layer inserted into an undoped semiconductor ridge waveguide nominally identical to the ones previously discussed and shown schematically in FIG. 2. While the waveguide serves to increase the interaction length of the laser fields with the weakly absorbing SAQDs the cavity aspect exploited in the PRDS is inconsequential in the spectral hole burning measurements. Photoluminescence data of the SAQDs in our samples (shown in FIG. 6) indicate a ground state transition wavelength of 1008 nm at a temperature of 10.0 K, while room temperature data (not shown) yield a ground state transition at 1150 nm. We also note that FIG. 6 indicates the inhomogeneous linewidth of the SAQD ensemble has a full width at half maximum (FWHM) of approximately 50 nm at 10.0 K. For spectral hole measurements the waveguides are mounted in a modified sample-in-vacuum $He^4$ flow cryostat with a base temperature of 9.8 K. At the experimental temperature the center wavelength for these measurements of 1064 nm ensures that the experiment examines only the ground state of the SAQDs. A schematic of the continuous wave spectral hole experimental setup is shown in FIG. 7. As it indicates in FIG. 7, the spectral hole measurements are performed by coupling light from two narrow-frequency external cavity diode lasers into the waveguide containing the SAQDs. The instantaneous linewidth for these lasers is less than 200 kHz, and we observe a heterodyne linewidth between the two lasers of $\sim$ 4 MHz for an integration time of $\sim$ 500 ms. The first of these sources remains at a fixed frequency and acts as the pump, burning a spectral hole in the inhomogeneous SAQD spectrum. The second beam serves as the probe and is swept in frequency relative to the pump. The collinear arrangement dictated by the waveguide geometry prevents the spatial discrimination of the probe signal from the much stronger pump light. Instead, signal discrimination is achieved by use of a heterodyne technique. The beam from the

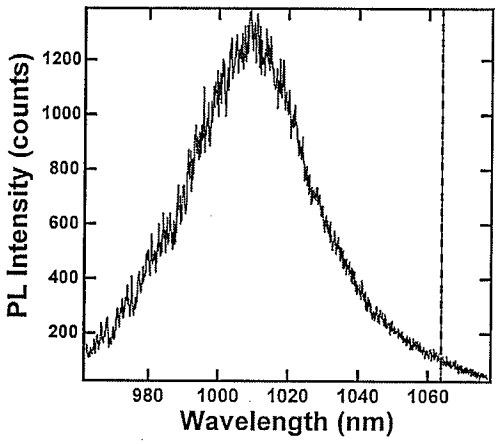


FIG. 6: Figure shows photoluminescence spectra taken at 10.0 K with an excitation power of 1.0 $\mu$W at 780 nm. The dashed line indicates the experimental wavelength of 1064 nm for the differential transmission measurements.

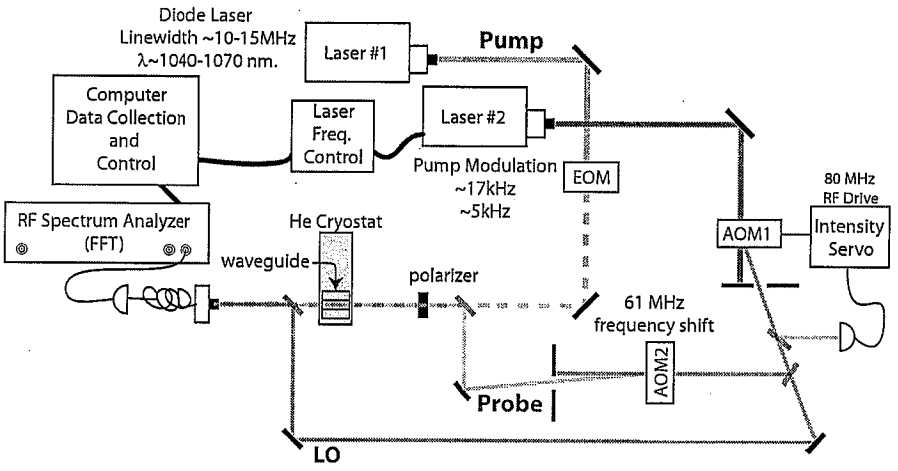


FIG. 7: Schematic of collinear continuous wave spectral hole burning setup. Laser #1 serves as a pump which is amplitude modulated using an electro-optic modulator, while the light from Laser #2 is split into a probe and local oscillator (LO) beams. The pump and probe pass through the semiconductor waveguide contained in a modified helium flow cryostat while the LO circumvents both the waveguide and cryostat. All three beams are couple through a single mode fiber to a InGaAs photodiode. The beat signal from the photodiode is then fed into a radio frequency lock-in or spectrum analyzer and then data are recorded via computer.

probe laser is split into two beams, one beam is frequency offset from the other by an amount $\omega_r \sim 61$ MHz with an acousto-optic modulator. This frequency shifted beam is coupled into the waveguide and serves as the probe. The unperturbed beam from the same source is routed to an InGaAs photodiode at the waveguide output. This beam serves as a local oscillator reference for the probe. The resulting probe/reference beat note in the photodiode at $\omega_r$ is free of any DC contamination from the pump . The pump is intensity modulated at a frequency $\omega_p \sim 17.1$ kHz with an electro-optic modulator. This second modulation at $\omega_p$ produces a differential transmission signal ($\Delta T/T$) that is observed as frequency sidebands on the probe/reference beat note at $\omega_r \pm \omega_p$.

This differential transmission signal is then recorded as a function of pump-probe laser detuning with a lock-in amplifier or directly with a radio frequency spectrum analyzer. The heterodyning of the probe and reference also provides amplification needed to observe the $\Delta T/T$ signal at the low probe beam powers that are required to limit self-broadening of the spectral hole. In all measurements reported here the pump and probe are linearly co-polarized and, consistent with previous reports, we observe the absorption signal only when the pump/probe polarization is perpendicular to the growth direction $z$ (12).

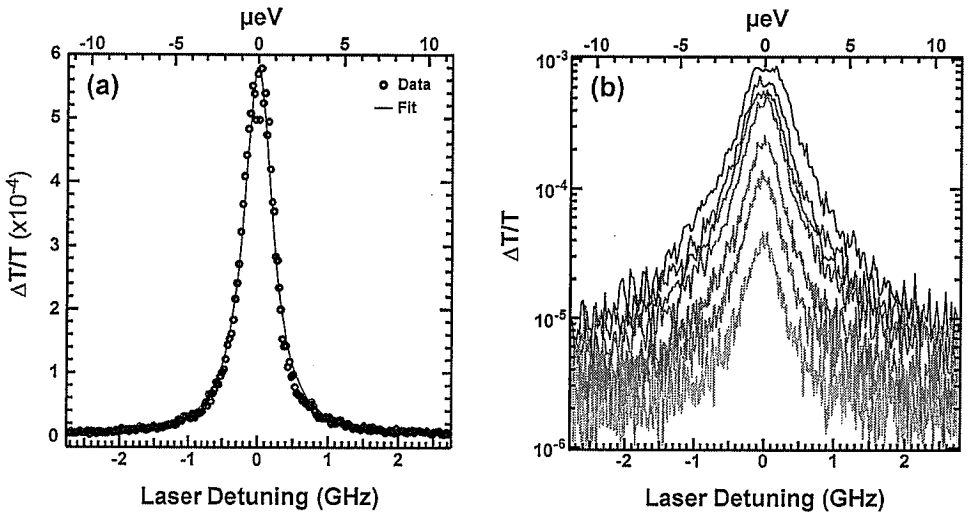


FIG. 8: Differential transmission signal ($\Delta T/T$) for single and multiple pump powers taken at 9.8K. Panel (a) shows the $\Delta T/T$ for a pump power of 77 pW, along with a Lorentzian fit to the data. Panel (b) shows selected $\Delta T/T$ data for pump powers ranging from 2.5 (bottom curve) to 208 pW (top curve). The data in panel (b) show a uniformity in the line shape, despite a clear increase in the line width with increasing pump power

The differential transmission data for an intermediate pump power are shown in FIG. 8 (a) along with a fit to a Lorentzian. We note that the Lorentizian fit to the $\Delta T/T$ signal is found to be numerically superior to a Voigtian line shape expected in the presence of inhomogeneous contributions. Unlike what is reported in other studies using this technique, we see no other evidence for either satellite peaks or the presence of inhomogeneous contributions to the lineshape. Panel (b) of FIG. 8 shows InGaAs SAQD differential transmission signals taken at 9.8 K for a range of pump powers, all of which also display a uniform Lorentzian line shape. In addition to the uniformity of the line shape, evidence of power broadening is also visible in the data in FIG. 8(b). The power broadening behavior of a two-level system is described by a square-root dependence of the linewidth with pump power (13, 14):

$$\Delta\omega_b = \Delta\omega_h(1 + P/P_0)^{\frac{1}{2}}. \qquad [4]$$

In equation [4], $\Delta\omega_b$ is the power broadened peak FWHM, $\Delta\omega_h$ is the homogeneous FWHM, $P$ is the pump power, and $P_0$ is the saturation pump power. A fit of the data to equation [4] permits the extraction of the homogeneous linewidth $\Delta\omega_h$ from the measured power broadened spectral hole linewidth $\Delta\omega_b$.

In FIG. 9 the FWHM is shown over an extended range of pump powers along with a fit to equation [4]. The corresponding energy widths may be calculated directly from $E = \hbar\omega$ and yields $\Delta E_h = 0.74 \pm 0.09$ $\mu$eV, or equivalently, $T_2 = 1.76 \pm 0.21$ ns (15). The values of the coherence time $T_2$ calculated from $\omega_h$ are shown in the bottom panel of FIG. 9. While the value of $P_0$ is subject to systematic errors and uncertainties in the pump power, such as the coupling efficiency, the value for the homogeneous FWHM $\omega_h$ is robust against pump power uncertainties. The uncertainties in $\omega_h$ result from changes in the pump-probe laser detuning and are reflected in the error bars of FIG. 9

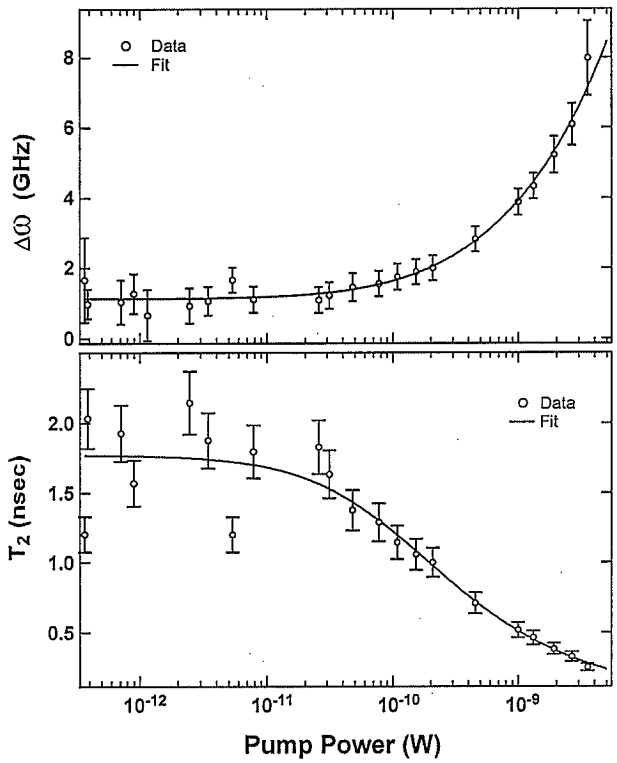


FIG. 9: Top panel shows spectral hole full width at half maximum ($\Delta\omega_b$) vs the pump power through the waveguide. Data are fit to $\Delta\omega_b = \Delta\omega_h(1+P/P_0)^{\frac{1}{2}}$ and yield $\Delta\omega_h = 1.13 \pm 0.14$ GHz and $P_0 = 90 \pm 30$ pW. Bottom panel shows the corresponding $T_2$ values vs pump throughput along with $T_2$ fit calculated from fit to $\omega_b$.

and the subsequently derived value for the coherence time. From time-resolved photoluminescence (TRPL) data shown in FIG. 10 we are able to determine the radiative recombination time for the SAQDs examined in our spectral hole measurement. A radiative lifetime of 970±100 ps was extracted by fitting the TRPL data with a single exponential convolved with the experimentally-determined instrument response. While the uncertainty in the instrument response limits the absolute accuracy, the 970±100 ps value for the lifetime gives a radiatively limited $T_2$ value of $1.9 \pm 0.2$ ns and indicates that the $T_2$ determined by our power broadening analysis is at or just below the radiative limit. Previous studies of InGaAs quantum dots have reported homogeneous FWHMs $\omega_h(\Delta E_h)$ in the range of 1.6-2.0 $\mu$eV, with corresponding coherence times $T_2$ between 680-830 ps (1, 3, 4). In contrast, our results indicate a significantly narrower energy width of $\Delta E_h < 1$ $\mu$eV and a correspondingly longer $T_2$, despite the fact that we are working at a higher experimental temperature. We believe that the difference between our measurement and those of previous reports arises from small but significant physical differences in the experimental methods and systems. For example, in reference (4) the time-resolved four-wave-mixing studies were carried out on a doped system, and due to the pulse bandwidth, a much wider section of the inhomogeneous linewidth (2 nm) was examined, in comparison to the narrow range considered here. By designing the experiment to probe a narrow frequency range at the ground state energies of the SAQDs, we circumvent dephasing mechanisms induced by the inhomogeneous distribution of dipole moments that will pollute the homogeneous lineshape and the subsequent $T_2$ value (16, 17). Other factors such as static electric fields or spectral diffusion, that may contribute to the observed spectral hole width, are mitigated by the intrinsic test structure and the underlying physics of the spectral hole burning technique (18).

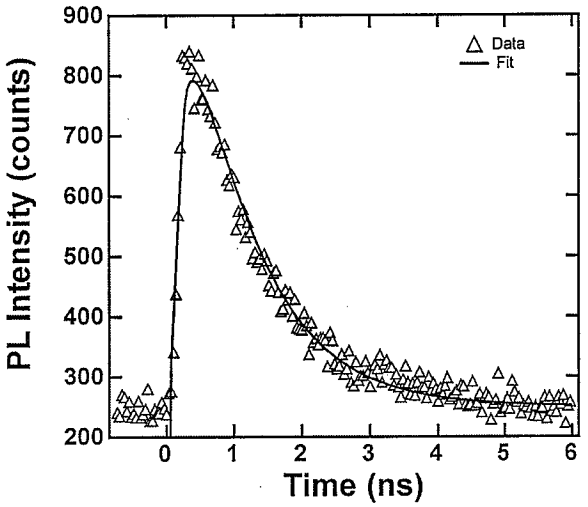


FIG. 10: Time-resolved photoluminescence data for SAQDs spectra at 1064 nm with a spectral resolution of 1.2 nm. Data were using a 1.0 $\mu$W average excitation power from a mode-locked Ti:Sapphire laser with a center wavelength of 780 nm and a 1.0 nm pulse bandwidth. Fit to data is a single exponential convolved with the instrumental response. Fit yields a radiative lifetime of 970±100 ps.

## IV. SUMMARY AND CONCLUSIONS

In this report we have demonstrated the efficacy of narrow line, high-resolution, absorptive spectroscopic techniques to examine the basic physical properties of InGaAs SAQDs. In the case of CWCRDS we examined the prospects for single SAQD spectroscopy with extremely high resolution using this technique. We successfully used this technique to characterize MBE-grown DBR mirrors and to observe absorption from SAQD ensembles. While our absorption sensitivity is not currently sufficient to examine a single SAQD absorber, analysis of the experiments indicates a minimum absorption sensitivity $\alpha_{min}$ of $3.35 \times 10^{-7}$ cm$^{-1}$. While significant technical barriers must be overcome in order to reach the sensitivity needed to examine a single SAQD, our current measurements give a true quantitative assessment of the potential of CRDS-based measurements to perform high precision spectroscopy on individual semiconductor nanostructures. We have also presented the novel application of spectral hole burning to perform high-resolution spectroscopy of SAQDs embedded in a ridge waveguide. This continuous wave pump-probe technique permits the differential transmission of a narrow energy range of SAQDs to be examined. The experimentally observed spectral holes are well fit by a Lorentzian lineshape and display power broadening behavior with increasing pump intensity. Analysis of the power broadening indicates a homogeneous FWHM of 0.74 $\mu$eV and a corresponding $T_2$ time of 1.76 ns. These results indicate a longer InGaAs/GaAs SAQDs coherence time compared with previously reported results.

We acknowledge contributions to this work by J. Ye, A. Marian, T. Harvey, M. Feng , J. Schlager and N. Brilliant.

(1) A. Högele, S. Seidl, M. Kroner, K. Karrai, R. J. Warburton, B. D. Gerardot, and P. M. Petroff, Phys. Rev. Lett. **93**, 217401 (2004).
(2) R. M. Stevenson, R. J. Young, P. Atkinson, K. Cooper, D. A. Ritchie, and A. J. Shields, Nature **439**, 04446 (2006).
(3) M. Bayer and A. Forchel, Phys. Rev. B. **65**, 041308 (2002).
(4) P. Borri, W. Langbein, S. Schneider, U. Woggon, R. L. Sellin, D. Ouyang, and D. Bimberg, Phys. Rev. Lett. **87**, 157401 (2001).
(5) A. O'Keefe and D. A. G. Deacon, Rev. Sci. Inst. **59**, 2544 (1998).

(6) R. W. P. Drever, J. L. Hall, F. V. Kowalski, J. Hough, G. M. Ford, A. J. Munley, and H. Ward, Appl. Phys. B **31**, 97 (1983).
(7) T. G. Spence, C. C. Harb, B. A. Paldus, R. N. Zare, B. Willke, and R. L. Byer, Rev. Sci. Instrum. **71**, 347 (2000).
(8) K. L. Silverman, R. P. Mirin, S. T. Cundiff, and A. G. Norman, Appl. Phys. Lett. **82**, 4552 (2003).
(9) J. Ye, Long-Sheng Ma, and J. L. Hall, J. Opt. Soc. Am. B **15**, 6 (1998).
(10) J. Ye and J. L. Hall, Phys. Rev. A. Rapid **61**, 061802 (2000).
(11) P. Palinginis, S. Tavenner, M. Lonergan, and H. Wang, Phys. Rev. B. **67**, 201307 (2003).
(12) K. L. Silverman, R. P. Mirin, S. Cundiff, and A. G. Norman, Appl. Phys. Lett. **82**, 4552 (2003).
(13) A. E. Siegman, *Lasers* (University Science Books, 55D Gate Five Road, Sausalito, CA 94965, 1986).
(14) L. Allen and J. H. Eberly, *Optical resonance and two-level atoms* (Dover Publications, 31 East 2nd Street, Mineola, NY 11501, 1987), 2nd ed.
(15) The relation between the FWHM $\Delta E_h$ and the coherence time $T_2$ is given by $\Delta E_h = \hbar\Delta\omega = 2\hbar/T_2$. In the radiative limit, the lifetime is half the coherence time ($T_1 = \frac{1}{2}T_2$).
(16) P. Borri, W. Langbein, S. Schneider, U. Woggon, R. Sellin, D. Ouyang, and D. Bimberg, Phys. Rev. B. **66**, 081306 (2002).
(17) P. Borri, W. Langbein, S. Schneider, U. Woggon, R. L. Sellin, D. Ouyang, and D. Bimberg, Phys. Rev. Lett. **89**, 187401 (2002).
(18) R. Oulton, J. J. Finley, A. D. Ashmore, I. S. Gregory, D. J. Mowbray, M. S. Skolnick, M. J. Steer, S. Liew, M. A. Migliorato, and A. J. Cullis, Phys. Rev. B. **66**, 045313 (2002).